Neurotherapeutics 21 (2024) e00436

Contents lists available at ScienceDirect

Neurotherapeutics

journal homepage: www.sciencedirect.com/journal/neurotherapeutics

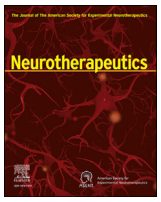

Original Article

Bioreactor-produced iPSCs-derived dopaminergic neuron-containing neural microtissues innervate and normalize rotational bias in a dose-dependent manner in a Parkinson rat model

Nicolas Prudon [a,b,*], Lucía Cordero-Espinoza [b], Myriam Abarkan [b], Basile Gurchenkov [b], Chloé Morel [b], Marilyn Lepleux [b], Valérie De Luca [b], Maxime Lartigue [b], Hélène Cabanas [b], Nadège Pujol [b], Loanne Milvoy [b], Pauline Morand [b], Fabien Moncaubeig [b], Hélène Wurtz [b], Léa Poinçot [b], Maëlle De Marco [b], Agathe Jonckeau [b], Justine Pletenka [b], Elisa Luquet [b], Andrea Sovera [b], Jérôme Hardoüin [b], Inês Januario Neves [b], Anaïs Machado-Hitau [b], Kathleen Schmit [b], Lucie Piouceau [b], Solenn Guilbert [b], Lucie Manache-Alberici [b], Michaël Lanero Fidalgo [b], Guillaume Dabée [a,c], Thibault Dufourd [b], Jens Schroeder [b], Kévin Alessandri [b], Erwan Bezard [a], Emilie Faggiani [b,1], Maxime Feyeux [b,1]

[a] Université de Bordeaux, CNRS, Institut des Maladies Neurodégénératives, UMR 5293, F-33000 Bordeaux, France
[b] TreeFrog Therapeutics, Bât A, F-33600 Pessac, France
[c] PIV-EXPE, Centre Broca, Université de Bordeaux, F-33000 Bordeaux, France

ARTICLE INFO

Keywords:
Cell therapy
Off-the-shelf
3D cell format
Midbrain
Organoid
Regenerative medicine

ABSTRACT

A breadth of preclinical studies now support the rationale of pluripotent stem cell-derived cell replacement therapies to alleviate motor symptoms in Parkinsonian patients. Replacement of the primary dysfunctional cell population in the disease, i.e. the A9 dopaminergic neurons, is the major focus of these therapies. To achieve this, most therapeutical approaches involve grafting single-cell suspensions of DA progenitors. However, most cells die during the transplantation process, as cells face anoïkis. One potential solution to address this challenge is to graft solid preparations, i.e. adopting a 3D format. Cryopreserving such a format remains a major hurdle and is not exempt from causing delays in the time to effect, as observed with cryopreserved single-cell DA progenitors. Here, we used a high-throughput cell-encapsulation technology coupled with bioreactors to provide a 3D culture environment enabling the directed differentiation of hiPSCs into neural microtissues. The proper patterning of these neural microtissues into a midbrain identity was confirmed using orthogonal methods, including qPCR, RNAseq, flow cytometry and immunofluorescent microscopy. The efficacy of the neural microtissues was demonstrated in a dose-dependent manner using a Parkinsonian rat model. The survival of the cells was confirmed by post-mortem histological analysis, characterised by the presence of human dopaminergic neurons projecting into the host striatum. The work reported here is the first bioproduction of a cell therapy for Parkinson's disease in a scalable bioreactor, leading to a full behavioural recovery 16 weeks after transplantation using cryopreserved 3D format.

Abbreviations: hiPSC, human induced pluripotent stem cells; PD, Parkinson's disease; STBR, stirred tank bioreactor; RT-qPCR, quantitative reverse transcription polymerase chain reaction; GMP, Good manufacturing practices; QC, Quality control; RNA, ribonucleic acid; NSC, neural stem cells; GFAP, glial fibrillary acidic protein; TH, tyrosine hydroxylase; DA, dopaminergic; cm, centimetre; mL, millilitre; rpm, rotations per minute; DO, dissolved oxygen; cDNA, complementary DNA.

* Corresponding author.
E-mail address: nicolas.prudon@u-bordeaux.fr (N. Prudon).

[1] These two authors contributed equally to this work.

https://doi.org/10.1016/j.neurot.2024.e00436
Received 10 February 2024; Received in revised form 14 August 2024; Accepted 14 August 2024

Introduction

In developing a cell therapy for Parkinson's disease (PD), numerous studies on foetal cell transplantation have provided valuable insights, particularly regarding long-term and robust clinical improvements observed in open-label studies [1–3]. The functional engraftment of transplanted tissue offers hope for advancing cell replacement strategies for PD with the potential to improve patients' lives significantly. However, the main challenge in foetal cell transplantation has been the limited and heterogeneous availability of source tissue [4]. The emergence of both embryonic stem cells and induced pluripotent stem cells (iPSCs) represents a potentially standardised and unlimited cell source, compatible with high-scale culture.

In 2009, the introduction of dual-SMAD inhibition opened new avenues for obtaining dopaminergic (DA) progenitors from human pluripotent stem cells (hPSCs) [5]. Subsequent demonstrations showcased the functionality of these cells in PD animal models [6–8]. Continuous refinement of neurodifferentiation protocols has since occurred to optimise product cell composition. Recent protocols have incorporated Good Manufacturing Practice (GMP) standards and quality controls (QC) to facilitate translation to the clinical phase [9–12]. Multiple initiatives using hPSC-derived DA progenitors are now entering the clinical trial phase [13].

The implication of using single-cell suspension is the risk of inducing programmed cell death through anoïkis [14], affecting the survival and/or the potency of the product post-transplantation. Employing an injectable 3D cell format - wherein neither detachment from cell culture vessels nor single-cell dissociation is required - would allow us to circumvent this limitation [10,15,16]. This format would provide protection, particularly for more mature and sensitive cells such as neurons [17]. Only one clinical-stage initiative has employed an injectable 3D format with DA progenitors. However, these cells were grafted fresh [10], as the cryopreservation of these 3D cell products remained challenging and resulted in a delayed time-to-effect [18]. Cryopreservation is crucial for ensuring the availability of precisely the same cell batches used in rigorous preclinical studies assessing safety and efficacy before transplantation into patients [4].

A key aspect impacting cell therapy availability is the bioproduction strategy. Currently, only scale-out methods [19,20], involving the multiplication of culture units in parallel have been employed [9–12]. These processes are prone to variability, as most are not automatised, relying on manual handling by operators, and are challenging to scale. While the scale currently demonstrated by others is sufficient for initiating a clinical trial [9–12], scalable solutions are crucial to address patient accessibility to cell therapies.

Bioreactors enable the scale-up of cell therapy processes developed in 2D systems, enhancing productivity and reducing costs [21]. Previously, we demonstrated that using alginate capsules allowed for the successful hiPSC amplification in Stirred-Tank Bioreactor (STBR), while maintaining stemness [22].

In this work, we describe the first STBR production of a cell therapy product for PD. We used our encapsulation technology [22–24] to produce midbrain patterned neural microtissues. The correct patterning of the microtissues was confirmed using orthogonal methods, including RT-qPCR, RNA sequencing, flow cytometry and immunofluorescence. The midbrain patterned neural microtissues comprised both DA progenitors and DA neurons. The absence of undifferentiated cells (hiPSC or neural stem cells (NSC)) or hindbrain/forebrain contaminants was confirmed. Finally, the transplantation of cryopreserved neural microtissues in a Parkinsonian rat model led to a behavioural recovery 16 weeks after transplantation.

Materials and Methods

Production of the neural microtissues

2D hiPSC culture

The hiPSC line (male) was provided by a GMP-qualified CRO and generated using cord blood derived $CD34^+$ progenitors. The hiPSC line was maintained on Vitronectin (StemCell Technologies, ref. 07180) and cultured in mTeSR1 medium (StemCell Technologies, ref. 85875). Cultures were fed daily, passaged with an enzyme-free reagent, ReLeSR (StemCell Technologies, ref. 05873) at 0,12 mL/cm^2 for 6 min at 37 °C every 3–4 days (around 80% confluency), and replated as small clusters (between 100 and 200 µm) at a density of about 20 000–40 000 cells/cm^2. Cells were cultured at 37 °C in a humidified atmosphere containing 5 % CO2. The last 2D cell culture passage (before encapsulation) was done using Accutase (StemCell Technologies, ref. 07920) at 0.08 mL/cm^2 for 6–8 min at 37 °C.

3D hiPSC encapsulation

Before encapsulation, 2D stem cell colonies were detached using Accutase (Stem Cell Technologies, ref. 07920). hiPSCs were resuspended in mTeSR1 medium (StemCell Technologies, ref. 85875) supplemented with 10 µM of Y-27632 (Tocris, ref. 1254). Cells were then mixed in a 1/1 vol ratio with human fibrinogen (Sigma Aldrich, ref. F3879-5G) and Y-27632 to reach final fibrinogen and Y-27632 concentrations of 14 mg/mL and 10 µM, respectively. The final concentration of cells in the cell/matrix solution was 3.6×10^6 viable cells/mL. The encapsulation system is similar to the one previously described [22–24], developed into a closed system. In brief, C-flex (Saint-Gobain, ref. 78413-25FT) and Pharmed tubings (Spetec, ref. 38-3232; ref. 38-3055) are connected to the three inlets of a 3D glass-printed microfluidic co-laminar flow device. A 3D glass-printed microcapillary tip (diameter of ~100 µm) is glued to the outlet of the nozzle for better control of the flow. The microfluidic co-laminar flow device and the microcapillary tip were printed using an SLE-based (Selective Laser Etching) 3D glass printer. The cell/matrix suspension is loaded into the inner channel of the 3-way device. A solution of 0.0147% SDS sodium alginate (Novamatrix, Pronova UP LG100 2%, ref. 4202171) is injected into the outer channel. To prevent alginate gelation within the microfluidic device due to calcium release from the suspended cells, a calcium-free solution (Sorbitol 300 mM, Sigma-Aldrich, ref. 85,529) is used in the intermediate channel of the co-extrusion chip. It serves as a barrier against calcium diffusion. This solution is supplemented with Thrombin (Proteintech, ref. HZ-3010) at a final concentration of 0.02 U/mL to allow for fibrin reticulation within the capsules. Typical flow rate for the 3 solutions was 80 mL/h for all three channels: the alginate solution, the sorbitol solution and the cell/matrix suspension. At these rates, the composite solution forms a liquid jet that fragments into droplets (about twice the size of the nozzle) due to the spontaneous Rayleigh-Plateau instability. To avoid coalescence of the train of droplets, the latter are charged to ensure their electrostatic repulsion. The alginate loading component and a stainless steel ring are connected respectively to a high voltage (1250 V) generator and to the ground. When the composite droplets contact the collecting 100 mM calcium bath, the outer layer of alginate readily gelates. Consequently, the inner cell/matrix solution get entrapped inside a closed, spherical and permeable micro-compartment. Within 3–5 min following the encapsulation, the capsules are rinsed with DMEM/F-12, HEPES 15 mM (Gibco, ref. 11330107) supplemented with 2.9 mM CaCl2, to reduce the basal calcium concentration. Finally, they are transferred into mTeSR1 medium supplemented with 10 µM Y-27632 as their initial suspension culture medium for neurodifferentiation.

3D hiPSC neurodifferentiation in bioreactors

Further neurodifferentiation was performed in a 500 mL bioreactor (Global Process Concept). The stirring speed was set at 150 rpm from day 0 to day 7, 200 rpm from day 7 to day 14, 230 rpm from day 14 to day 18 and 250 rpm from day 18 to day 24. The bioreactors were provided with 25 % (V/V) capsule-to-medium volume. In the 500 mL bioreactor, the culture volume was maintained at 300 mL during the whole culture. At day 1, the medium was completely renewed with fresh medium supplemented with ROCK inhibitor. At day 2, no media change was performed. At day 3, the medium was completely renewed, with fresh medium without ROCK inhibitor. From this day onwards, media change

was performed in perfusion. At day 12, 13 and 18, the medium was completely renewed with fresh medium. The final capsule-to-medium volume was between 22 % and 25 %. The pH was maintained at 7.2 ± 0.2. The dissolved Oxygen (DO) level was calibrated at 100 % both before and after the autoclave in the empty bioreactor and in the starting conditions (filled with media), respectively. During the run, the oxygen level was monitored and controlled at 50 % DO by sparging oxygen.

Molecules were added as follows: From day 0, mTeSR1 medium (Stemcell Technologies, ref. 85875) was supplemented with 10 µM Y-27632 (Tocris, ref. 1254) for ROCK inhibition for the first 48 h of culture. mTeSR1 medium was kept until day 3. Recombinant Human Noggin GMP Protein (R&D Systems, ref. 6057-GMP 01 M) was initially added at day 0 (encapsulation day) at a concentration of 60 ng/mL and gradually increased at day 1 and day 2 as 84 ng/mL and 100 ng/mL respectively. Similarly, SB431542 GMP (R&D Systems, ref. TB1614-GMP/10) was initially added at 0.2 µM on day 0, and gradually increased at 2 µM and 20 µM at day 1 and day 2, respectively. On day 3, the medium was changed for Neurobasal™ CTS™ (Gibco, ref. A1371201) and DMEM/F-12, supplement GlutaMAX™ (Gibco, ref. 31331-028) in a ratio 1:1 (V/V), supplemented with N-2 Supplement CTS™ (Gibco, ref. A13707-01) and B-27™ Supplement GMP (Gibco, ref. A33535-01). From day 3 to day 12, 100 ng/mL recombinant human Noggin GMP protein, 20 µM SB431542 GMP, 100 ng/mL recombinant human Sonic Hedgehog/Shh (C24II) N-Term GMP (R&D Systems, 1845-GMP-500), 100 ng/mL HumanKine® recombinant human FGF-8b protein (Miltenyi, ref. 130-095-741) and 2 µM StemMACS Purmorphamine (Miltenyi Biotec, ref. 130-104-465) were added. CHIR99021 GMP (R&D Systems, ref. TB4423-GMP/10) was added from day 6 up to day 13. Afterward, 200 µM Ascorbic acid (Sigma Aldrich, ref. 1043003-1G), 10 ng/mL recombinant human GDNF GMP Protein (R&D Systems, ref. 212-GMP-01 M), 1 ng/mL HumanKine® recombinant human TGF-beta 3 Protein (Proteintech, ref. HZ-1090), 5 ng/mL recombinant human FGF-20 Protein (R&D Systems, ref. 2547-FG-025), 0.5 mM Dibutyryl cAMP (Sigma, ref. D0627), 10 µM DAPT RMU (R&D Systems, ref. TB2634-RMU/10), 1 µM Compound E (Tocris, ref. 6476/1) and 10 nM Trichostatin A (Sigma Aldrich, ref. 647925-1 MG) were added from D13 to D17. Finally, 20 ng/mL HumanKine® recombinant human BDNF protein (Miltenyi, ref. 130-103-435) was added from day 13 to day 24. Neural microtissues were then harvested on day 24, decapsulated and cryopreserved using a Controlled Rate Freezer (Thermo Scientific, CryoMed Model-7450) and Bambanker hMR (Nippon Genetics, ref. BBH01) as a cryoprotective agent.

Characterization of neural microtissues

RNA extraction and RT-qPCR analyses

Samples were homogenised in Tri-reagent (Euromedex, ref. TR 118-200) and RNA was isolated using a standard chloroform/isopropanol protocol [25]. RNA was processed and analysed following an adaptation of published methods [26]. cDNA was synthesised from 2 µg of total RNA using Maxima Reverse Transcriptase (Fisher Scientific, ref. 10420100) and primed with oligo-dT primers (Fisher Scientific, ref. 10753741) and random primers (Fisher Scientific 10580091). QPCR was performed using a LightCycler® 480 Real-Time PCR System (Roche). QPCR reactions were duplicated for each sample, using transcript-specific primers, cDNA (4 ng) and LightCycler 480 SYBR Green I Master (Roche) in a final volume of 10 µl. For the determination of the reference gene, the RefFinder method was used [27]. Relative expression analysis was normalised against five reference genes if no specific reference gene is mentioned. Proteasome subunit beta 4 (*PSMB4*), non-POU domain containing octamer binding (*NONO*), chromosome 1 open reading frame 43 (*CLORF43*), Tyrosine 3-Monooxygenase/Tryptophan 5-Monooxygenase Activation Protein Zeta (*YWHAZ*) and Actin beta (*ACTB*) genes were used. The PCR data were exported and analysed in an informatic tool (Gene Expression Analysis Software Environment) developed at the NeuroCentre Magendie. The relative level of expression was evaluated by calculating $2^{\Delta Ct} = 2^{(Ct(\text{gene of interest}) - Ct(\text{mean value of the 5 reference genes}))}$. Primers sequences are reported in the supplementary data (supplementary Table S1).

Flow cytometry analysis

Neural microtissues were harvested at several neurodifferentiation time points. The alginate capsule was removed by incubating the sample for 5 min in RelesR (StemCell Technologies, ref. 05873) at room temperature with a final concentration of 20 % capsules (V/V). After RelesR wash, neural microtissues were then dissociated using the Neurosphere dissociation kit (Miltenyi Biotec, ref. 130-095-943) for 40 min at 37 °C with agitation (150 rpm) and manual resuspension using a micropipette every 10 min. Then, cells were fixed and permeabilised using the Fixation/Permeabilisation Concentrate (ThermoFisher, ref. 00-5123-43) and the Fixation/Permeabilisation Diluent (ThermoFisher, ref. 00-5223-56) in a 1:4 ratio, at a maximum cell density of 5.10^6 per mL. Cells were then resuspended in the Flow cytometry staining buffer (ThermoFisher, ref. 00-4222-26) at 833,333 x 10^3 per mL cell density. Cells were centrifugated at 500 g for 5 min at room temperature, and the supernatant was removed. Samples were then incubated for 30 min in the dark at room temperature, with the specific antibodies (supplementary Table S2) diluted at 1:50 in Permeabilisation Buffer 1X (Invitrogen, ref. 00-8333-56). The samples were finally washed twice by performing centrifugations at 500 g for 5 min at room temperature and resuspending the cells with the staining buffer. The samples were analysed using MACSQUANT® Analyser 10 (Miltenyi Biotec). Isotype controls were performed to determine the limit of positivity above which a sample will be considered positive and validate the antibodies specificity. Compensation controls for each fluorochrome were used to remove spectral overlap. Data was post-processed with FlowJo analysis software versions 10.8 and 10.9. Gating was performed by using unstained cells as a negative control to differentiate stemness-specific or neural-specific antibody labelling and non-specific background signals. Significant signals of both NANOG+/OCT4+, SSEA5+/SSEA4+ and TRA-1-60+/OCT + populations are therefore used to identify and calculate the percentage of pluripotent cells. Signals of both PAX6+/SOX1+ or FOXA2+/OTX2+ populations are used to respectively identify and calculate the percentage of neural stem cells and dopaminergic progenitors in the sample.

Immunolabelling, microscopy and image analysis

For daily brightfield imaging of 2D cultures and encapsulated neural microtissues, a widefield EVOS M5000 microscope was used. Encapsulated 3D neural microtissues were harvested for observation using confocal microscopy at several time points. The alginate capsule was removed by incubating the sample for 5 min in RelesR (StemCell Technologies, ref. 05873) at room temperature with a final concentration of 20 % capsules (V/V). Three-dimensional stem cell colonies were fixed with 4% PFA for 1h at room temperature in the dark. Following fixation, the samples were washed 3 times with 0.1% Tween20 in PBS. A permeabilisation step was done in a PBS solution containing 5 % Triton X-100 for 30 min under agitation (170 rpm) at room temperature. Samples were washed 3 times with 0.1% Tween20 in PBS. The samples were incubated in adequate primary and secondary antibodies 0.1% Tween20 in PBS 72 h at room temperature under agitation (170 rpm). Samples were rinsed five times with 0.1% Tween20 in PBS after each incubation, including two rinses under agitation for 30 min at 170 rpm. Samples presented in Fig. 2 D.a, D.c and D.d, as well as in supplementary data were imaged with a motorised widefield fluorescent microscope (Leica Microsystems, THUNDER Imager Live Cell, ref. 11525681) and automatically deconvoluted. The sample presented in Fig. 2 D.b was imaged with a confocal microscope (Leica Microsystems, DM6000 TCS SP5 MP).

Dopamine measurement by LC-MS/MS

After 24 h of culture at the end of the neurodifferentiation process (culture day 25), fresh neural microtissues were washed twice with low

KCl solution (20 mM HEPES, pH 7.4, 140 mM NaCl, 4.7 mM KCl, 2.5 mM CaCl2, 1.2 mM MgSO4, 1.2 mM KH2PO4, and 11 mM glucose) and then incubated in either low KCl solution supplemented in citric acid at 0,1 mg/mL for 1 h or in high KCl solution (20 mM HEPES, pH 7.4, 85 mM NaCl, 60 mM KCl, 2.5 mM CaCl2, 1.2 mM MgSO4, 1.2 mM KH2PO4, and 11 mM glucose) supplemented in citric acid for 1 h at 37 °C. The conditioned medium was then collected, and the dopamine concentration was determined by LC-MS/MS (Acquity UPLC and Xevo TQ-XS mass spectrometer). Data were calculated from independent experiments using 4 different bioreactors.

Viability assay

Cells were thawed by gently shaking the cryotube in a water bath (Grant Instruments LTD, ref. JBN12) at 37 °C. Once a small ball of ice was remaining (approximately after 2 min), the cells were rinsed twice with 0.004% Tween80 (AVANTOR, ref. 4117-04) PBS (Gibco, ref. 14287-080) and once with Neurobasal™ CTS™ (Gibco, ref. A1371201) and DMEM/F-12, supplement GlutaMAX™ (Gibco, ref. 31331-028) in a ratio 1:1 (V/V), supplemented with N-2 Supplement CTS™ (Gibco, ref. A13707-01) and B-27™ Supplement GMP (Gibco, ref. A33535-01). The cells were then stained using a Live Dead Viability/Cytotoxicity Kit (Invitrogen, ref. L3224) following the manufacturer's recommendations. A positive control for cell death was also performed by heating the cells at 65 °C for 10 min using a ThermoMixer C (Eppendorf, ref. 5382000.015). Cells were finally imaged using an EVOS™ M5000 Imaging System (Invitrogen, AMF5000).

In vivo study

Animals and stereotactic lesion surgery

Adult male Rowett nude rats (Rnu) (7.5–9.5 weeks, Charles River) were housed in a 12-hr-light/dark cycle temperature and humidity-controlled room with *ad libitum* access to food and water. All experiments were performed per French guidelines (87-848, Ministère de l'Agriculture et de la Forêt) and the European Community Council Directive (2010/63/EU) for the care of laboratory animals. Animal experiments were approved by the Institutional Animal Care and Use Committee of Bordeaux (CE50) under license number APAFIS #22371-2019101015375218 v3.

For the lesion induction, animals were anaesthetised using an induction chamber at 4% isoflurane (parameters of the induction chamber: i4 Oxy1 Air1). Rats were then placed on an anaesthesia mask, using approximately 2.5% isoflurane (parameters of the induction chamber: i2.5 Oxy0.4 Air0.4). Concentration could be slightly adjusted by manually regularly checking paws and body temperature. Analgesia was performed by subcutaneously injecting. Buprenorphine and Lidocaïne at respective concentrations of 0.05 mg/kg and 5 mg/kg. Rats were intraperitoneally injected with additional Hydrochloride desipramine at a concentration of 25 mg/kg at least 20 min before 6-hydroxydopamine hydrobromide (6-OHDA/HBr) injection. 2.5 µL of freshly prepared 6-OHDA/HBr at a concentration of 0,5 % (w/v) was infused in the Median Forebrain Bundle (MFB) using a stereotaxic frame with the coordinates (Bregma as reference): AP: −3.8; ML (right): −1.6; DV: from −8 to −7. After minimum 3 weeks of lesion stabilisation, behaviour was assessed using the Amphetamine-induced rotation tester.

Amphetamine-induced rotation test

Amphetamine-induced rotation behaviour was evaluated before (minimum 3 weeks after 6-OHDA injection) and every 4 weeks after the transplantation. The number of rotations was recorded in an automated rotational bowl as previously described [28], 10 min after an intraperitoneal injection of Amphetamine (2.5 mg/kg) for 40 min. The results are presented in rotation/min. Only rats that showed more than 4 rotations per minute after lesion stabilisation were included into the behavioural analysis.

Stereotactic transplantation of neural microtissue

On the day of the transplantation, cells were thawed by slowly shaking the cryotube in a water bath (Grant Instruments LTD, ref. JBN12) at 37 °C. Once a small ball of ice was remaining (approximately after 2 min), the cells were rinsed twice with culture medium. The cells were finally resuspended in a custom-made administration medium composed of hyaluronic acid and dextran 40 kDA (HA100-DA40) and injected into the right striatum of rats using a 25 µL Hamilton (Hamilton, ref. 1702 CX SYR) with custom-made needles (glass cannula). Anaesthesia and analgesia procedures are the same as the one described above for stereotactic lesion surgery. The injection was performed in two trajectories using a stereotaxic frame and the following coordinates (Bregma as reference): 1st trajectory: AP: +0.5, ML: −3, DV: −6 to −4; 2nd trajectory: AP: +1, ML: −2.5, DV: −6 to −4. At the end of the surgery, Metacam was subcutaneously injected at a concentration of 1 mg/kg for postoperative pain management.

Post-mortem histological analysis

Animals were anesthetised by intraperitoneally injecting ketamine (100 mg/kg) and xylazine (20 mg/kg). Animals were then intra-cardially perfused with 150 mL of 0.9% NaCl, followed by 200 mL of Formalin 10% Buffered in phosphate (Electron microscopy biosciences, ref. 15740) at a flow rate of 25 mL/min. Rodents were then decapitated, and the brain was collected. After extraction, brains were post-fixed in Formalin 10% Buffered in phosphate for 24h at 4 °C and finally stored in PBS (Thermo Fisher Scientific, ref. 14190094) at 4 °C. Sections at 40 µm were collected using a vibratome (Leica, Ref. VT1000S) and stored in 0.01% Azide (Sigma Aldrich, ref. 71289) PBS. They were washed 3 times with PBS (Thermo Fisher Scientific, ref. 14190094). Then, they were permeabilised by incubating 1h at room temperature in 0.1% Triton 2% BSA PBS and washed 3 times with PBS. They were then stained for tyrosine hydroxylase (TH 1:1000, Abcam, ref. ab112) and human antigen (Stem121 1:1000, Takarabio, ref. Y40410) by incubating primary antibodies in 0.05% Triton 0.5% BSA PBS overnight at 4 °C. They were washed 3 times with PBS. Sections were then incubated with fluorochrome-conjugated (Alexa 488, 568) secondary antibodies (1:1000, Invitrogen, ref. A11034; A11031) in 0.05% Triton 0.5% BSA PBS for 2 h at room temperature. After rinsing 3 times with PBS, sections were mounted on slides using DAPI Fluoromount-G (Clinisciences, ref. 0100-20), counterstaining the nuclei. Finally, slides were imaged using a slide scanner (Hamamatsu, ref. Nanozoomer 2.0HT). The images were segmented in the TH channel by thresholding, then binarized and skeletonised in Fiji/ImageJ [29], to highlight the projections from the graft.

Statistical analysis

All statistical analyses were performed using GraphPad Prism 10.1.1. For flow cytometry, Sidak's multiple comparison tests were performed (****$p < 0.0001$). For *in vitro* TH + cells quantification and transplanted TH + cells quantifications, analyses were performed using Welch's *t*-test (***: $p < 0.001$, ****: $p < 0.0001$). For behavioural analyses, comparisons were made to the vehicle group using Two-Way ANOVA and Tuckey's multiple comparison test (***: $p < 0.001$, ****: $p < 0.0001$).

Data availability

The data supporting the findings of this study are available from the corresponding author upon reasonable request.

Results

Scalable bioproduction of ventral midbrain DA microtissues and in vitro characterisation

We encapsulated hiPSC as previously described [22] and differentiated them into ventral midbrain dopaminergic neural microtissues.

Briefly, hiPSC were encapsulated into hollow alginate capsules using a microfluidic chip [23] (Fig. 1A a). The encapsulated cells were cultured inside a 500 mL bioreactor and neuro-differentiated (Fig. 1A b). Neural induction was performed via dual SMAD inhibition [5] and the cells were further patterned to a midbrain identity using CHIR99021, SHH, Purmorphamine and FGF-8b. Finally, the cells were exposed to maturation factors, including BDNF, GDNF, TGF-Beta3, FGF-20, dbcAMP, DAPT, Compound E and Trichostatin A. This process leads to the production of neural microtissues with an approximate diameter of 200 µm, achieved after a total culture duration of 24 days (Fig. 1B and C). The neural microtissues are then harvested and cryopreserved after removal of the alginate capsule (Fig. 1A c). Gene expression analysis of 13 different production batches (Fig. 2A) confirmed the significant enrichment of RNA transcripts associated with the midbrain region (*OTX2, LMX1A, FOXA2, CORIN, EN1* and *PAX8*). The decrease of pluripotent stem cell gene expression was also confirmed by *POU5F1* and *NANOG* expression. The *SOX1* and *PAX6* RNA transcripts were enriched compared to pluripotent stem cells. This increased expression could correspond to the remaining NSC. The increase in *PAX6* RNA transcripts alone could also correspond to forebrain contaminants. We also detected the enrichment of more mature neuronal RNA transcripts, like *MAP2*, *TUBB3*, *SYN1* and *TH*, potentially tracing the emergence of a more mature cell population within the microtissue, which could include dopaminergic neurons. The expression of *GAD1* was detected and increased compared to hiPSCs, suggesting the potential presence of GABAergic neurons within the microtissues. On the opposite, the expression of *TPH2* was not increased, which does not support the presence of serotonergic neurons within the product. The expression of *COL1A1*, associated with vascular leptomeningeal cells (VLMCs) in grafts derived from DA progenitor transplantation [30] and in extended cultures of midbrain organoids [31] was decreased compared to hiPSCs, strongly suggesting the absence of VLMCs within the neural microtissues. The expression of *GFAP* in the final microtissue (D24) was below the detection threshold (supplementary Fig. S1) for several bioreactors (n = 6/13), suggesting that the increase in the fold change observed between D0 and D24 might not be relevant (Fig. 2B). The absence of astrocytes within the neural microtissue at D24 was confirmed at the protein level (Fig. S8). The expression of *OLIG2* was above the detection threshold and increased compared to hiPSCs (supplementary Fig. S1), suggesting the potential presence of oligodendrocytes. Finally, the expression of *PCNA* and *KI67* was like the hiPSCs, indicating the presence of proliferative cells. These proliferative cells could correspond to dopaminergic progenitors due to the significant increase in the associated transcription factors RNA transcripts *(OTX2, LMX1A and FOXA2)*. This gene expression profile was confirmed using bulk RNAseq on the batch used for *in vivo* transplantation, both on fresh and cryopreserved cells (Fig. 2B). The absence of RNA transcript enrichment from forebrain (*FOXG1*), hindbrain (*GBX2, MAFB, EGR2, HOXA2, HOXB1, HOXA3, HOXB2, HOXA4*) or spinal cord (*HOXB8, HOXC10*) contaminants was further confirmed.

Next, we used flow cytometry to examine the cells obtained at the protein level. After microtissue dissociation, the cells from 13 different batches were stained using a panel designed to characterise the potential remaining hiPSCs (SSEA4/SSEA5; OCT/NANOG and TRA-1-60/OCT) or NSCs (PAX6/SOX1) (Fig. 2C). The presence of hiPSCs was negligible with 0.07% ± 0.06% OCT/NANOG; 0.28% ± 0.35% SSEA4/SSEA5 and 0.50% ± 0.39% TRA-1-60/OCT double positive cells. The presence of

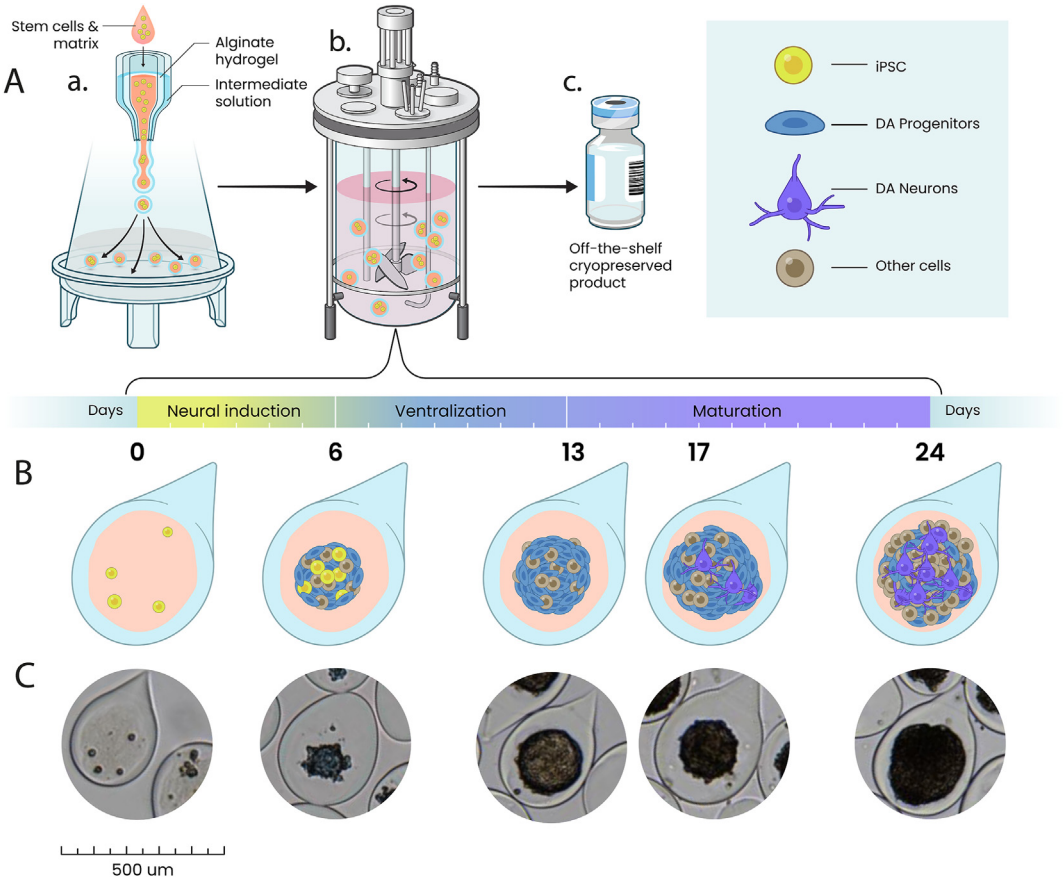

Fig. 1. Schematic overview of the neural microtissues bioproduction process. A: (a) hiPSCs were encapsulated using a microfluidic chip. (b) Cells were further cultured and differentiated in a 500 mL bioreactor. The neurodifferentiation protocol is illustrated with schematic neural microtissues and the corresponding widefield microscope pictures. (c) At harvest, the microtissues were decapsulated and cryopreserved using a CRF (Controlled Rate Freezer). B: Schematic representation and C: corresponding widefield microscope pictures of the neural microtissues across the neurodifferentiation protocol. Scale bar: 500 µm.

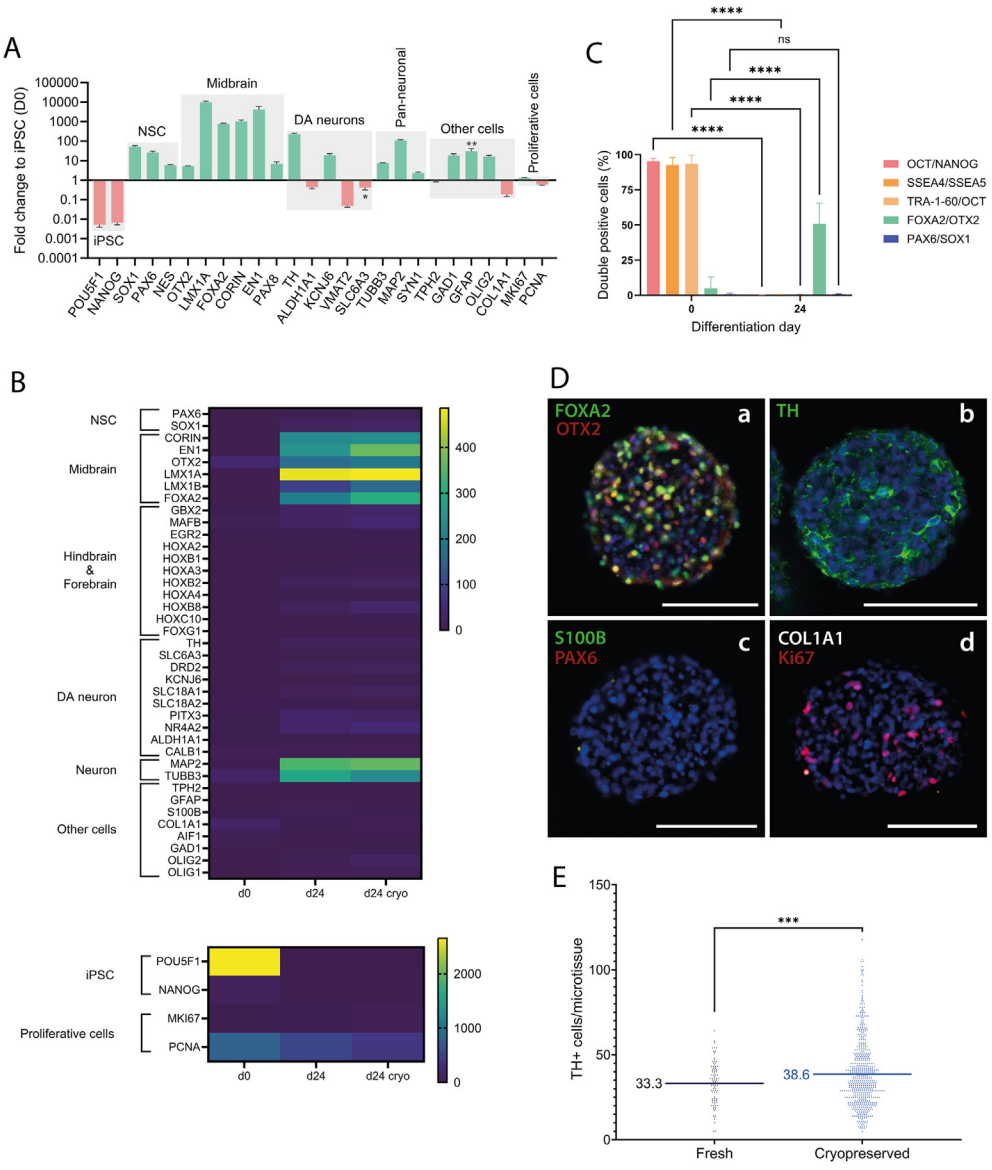

Fig. 2. *In vitro* characterisation of the neural microtissues. A. Gene expression analysis of the fresh neural microtissue using bulk RT-qPCR. Values are represented as fold change to hiPSC (D0). Experiments were performed in technical duplicates. Data are presented as histograms (n = 13 batches). Error bars are SEM. Raw expression values for the genes *SLC6A3* (*) and *GFAP* (**) were below the detection threshold ($2^{\Delta Ct} < 10^{-4}$) for a fraction of the bioreactors analysed (*n = 5/13, **n = 6/13). Raw values are also plotted in the supplementary data (supplementary Fig. S1). B. Transcriptomics analysis of the starting hiPSC (D0), the fresh and the cryopreserved neural microtissue (D24) from the transplanted batch. The gene expression profile described in the qPCR analysis was confirmed, along with no enrichment of gene expression associated with potential forebrain (*FOXG1*), hindbrain (*GBX2, MAFB, EGR2, HOXA2, HOXB1, HOXA3, HOXB2, HOXA4*) or spinal cord (*HOXB8, HOXC10*) contaminants. Data are represented as TPM (transcript per million). C. Flow cytometry analysis of fresh single cells from the encapsulation day D0 (hiPSC) or at the end of the bioproduction process D24 (dissociated neural microtissue). An antibody panel was used to identify pluripotent stem cells (OCT/NANOG; SSEA4/SSEA5 and TRA-1-60/OCT), neural stem cells (PAX6/SOX1) and DA progenitors (FOXA2/OTX2). Data are presented as histograms (n = 13 batches) and analysed with Sidak's multiple comparison test; error bars represent SD. ****p < 0,0001. D. Immunofluorescence images of cryopreserved neural microtissues from the transplanted batch (a–d). Cryopreserved neural microtissues were thawed and then fixed before the immunolabelling. Dopaminergic progenitors were detected using the markers FOXA2 and OTX2 (a) along with more mature dopaminergic neurons positive for TH (b). The absence of astrocytes and neural stem cells was confirmed, using the markers S100B and PAX6, respectively (c). No VLMCs were detected in the neural microtissues using the marker COL1A1, and cells remaining in the cell cycle were detected as positive for the marker Ki67 (d). Samples were counterstained with DAPI (a–d). Scale bar: 100 μm. Splits of the colour channels are available in the supplementary data (supplementary Figs. S2–8). E. *In vitro* quantification of DA neurons using immunofluorescence images from the transplanted batch. The numbers of TH + cells were quantified in fresh (n = 87) and cryopreserved (n = 555) microtissues. Data are represented as mean in scatter-plot and analysed using Welch's *t*-test. ***: p < 0,001. (For interpretation of the references to colour in this figure legend, the reader is referred to the Web version of this article.)

NSC was confirmed also to be less than 1% of the cells, with 0.72% ± 0.42% double positive for PAX6/SOX1. This suggests that the increase in PAX6 expression detected at the transcript level using qRT-PCR may not be sufficient to translate into significant protein expression. The proper patterning of the neural microtissues was confirmed with approximately half of the cell population (50.8% ± 14.8%) double positive for midbrain dopaminergic markers (FOXA2/OTX2).

Since the dissociation of 3D cell format into single cell suspensions is expected to induce a bias in cell composition [32], we opted for immunofluorescence labelling as a complementary characterisation method on

the batch used for *in vivo* transplantation. As expected and consistent with the qPCR results, the presence of midbrain dopaminergic progenitors was confirmed by the FOXA2/OTX2 labelling (n = 15, Fig. 2D a, supplementary Fig. S2), in conjunction with more mature neuronal cells expressing MAP2 (n = 15, supplementary Fig. S3). Some cells expressed the dopaminergic marker TH (n = 555, Fig. 2D b, supplementary Fig. S4). The absence of NSC or forebrain progenitors was confirmed by the absence of PAX6 labelling (n = 7, Fig. 2D c, supplementary Fig. S5), consistent with flow cytometry results. The absence of remaining undifferentiated hiPSCs was confirmed by the lack of NANOG detection (n = 15, supplementary Fig. S6). No VLMCs could be detected as confirmed by the markers COL1A1 (n = 15, Fig. 2D d, supplementary Fig. S7). The absence of astrocytes was confirmed with the absence of any S100B (n = 7, Fig. 2D c, supplementary Fig. S5), SOX9 or GFAP-positive cells (n = 9, supplementary Fig. S8). This confirms that the low expression of *GFAP* observed at the transcriptomics level did not translate into protein expression. The absence of oligodendrocytes was also confirmed by the analysis of the marker OLIG2 (supplementary Fig. S3). This suggests that the gene expression of *OLIG2* previously detected with qPCR may not be sufficient to translate into protein expression. The presence of remaining proliferative cells was also confirmed using the marker Ki67 (Fig. 2D d, supplementary Figs. S6 and S7). Next, we counted the number of TH + cells per neural microtissue to establish a dose rationale in the preclinical study. The means were 33.2 ± 12.6 and 38.6 ± 19.8 TH + cells per microtissue, for fresh (n = 87) and cryopreserved microtissues (n = 555), respectively (Fig. 2E). To assess the functionality of the TH + cells,

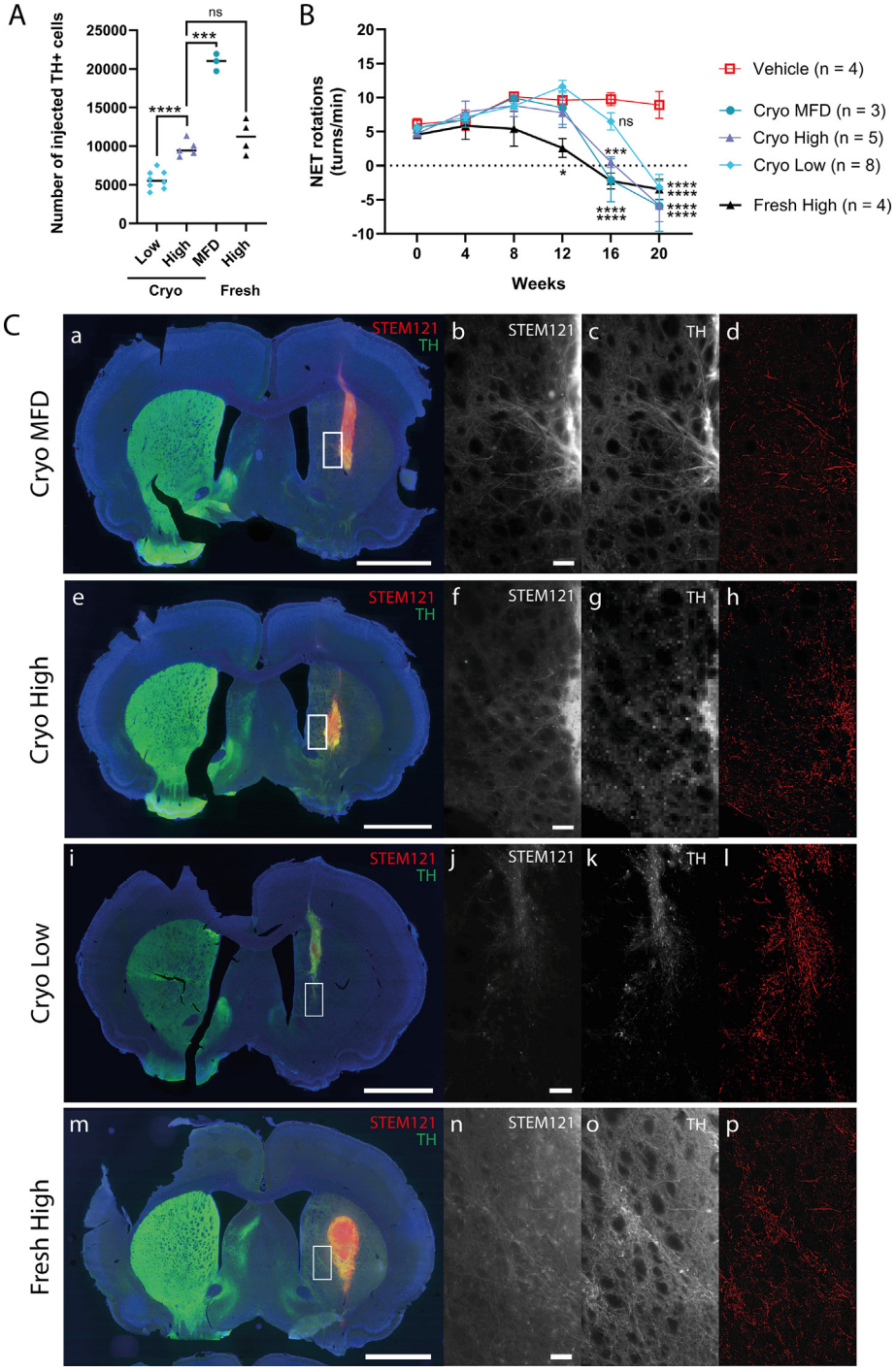

Fig. 3. Non-clinical efficacy study of neural microtissues in the hemiparkinsonian rat model. A. Distribution of animals in the different dose groups based on the estimated number of injected TH + cells. The total number of injected TH + cells per animal was calculated by the number of neural microtissues injected and the number of TH + cells per microtissue (n = 15) specific to each cryovial. Data are presented as mean in a scatter plot and analysed using Welch's *t*-test (***: $p < 0.001$, ****: $p < 0.0001$, ns: not significant). B. Time-based analysis of d-amphetamine-induced rotations measured pre-operatively and 4, 8, 12, 16 and 20 weeks (n = 16) post-engraftment. The graft of neural microtissues achieved functional recovery of motor deficits 16 weeks after transplantation for the Fresh High (n = 4, $p < 0,0001$), the Cryopreserved High (n = 5, $p < 0.0001$) and the Cryopreserved Maximum Feasible Dose (MFD) (n = 3, $p < 0.0001$), corresponding to a total of 11 000 TH + cells transplanted for both fresh and cryopreserved High doses and 21 000 TH + cells for the MFD. A delay was observed for the Low dose group, corresponding to 6000 TH + cells transplanted, with full functional recovery observed 20 weeks after transplantation (n = 8, $p < 0.0001$). Comparisons were made to the vehicle group using Two-Way ANOVA and Tuckey's multiple comparison test (*: $p < 0.05$, ***: $p < 0.001$, ****: $p < 0.0001$, ns: not significant). Data are presented as mean ± SEM. C. Post-mortem histological analysis of the graft. Representative sections of animals 20 weeks after receiving the cryopreserved Maximum feasible dose (a–d), cryopreserved High dose (e–h), cryopreserved Low dose (i–l) or Fresh High dose (m–p). Sections were immunostained for the human marker Stem121 (b, f, j, n) and TH (c, g, k, o). Merges (a, e, i, m). Image analysis of the TH-immunolabeling was performed to better highlight reinnervation using skeletonisation (d, h, l, p). Rectangles show areas of magnification shown in the right panels, illustrating dopaminergic projections from the graft. Scale bars: 2,5 mm (a, e, i, m) and 100 μm (b-d, f-h, j-l and n-p).

dopamine release was measured in additional bioproduction lots. Dopamine was quantified via liquid chromatography with tandem mass spectrometry (LC-MS-MS) using conditioned medium from fresh neural microtissues at the end of the neurodifferentiation process. Functional release of dopamine was detected, with concentrations ranging from 2.8 to 29.45 ng/mL of microtissues. Finally, the viability of the cryopreserved neural microtissues after thawing was confirmed using a calcein AM/ethidium homodimer 1-based viability assay (supplementary Fig. S9).

Dopaminergic neural microtissues dose-dependently restore the motor function of a Parkinson's rat model

To evaluate the potential efficacy of the neural microtissues, we unilaterally injected different cryopreserved doses of neural microtissues and one fresh dose as the control into the striatum of lesioned athymic nude rats. Rats with unilateral 6-OHDA-induced medial forebrain bundle (MFB) lesions confirmed by repeated d-amphetamine-induced rotations were transplanted with vehicle control (n = 4) or cryopreserved Low dose (9 x 10^3 TH + cells; n = 8), cryopreserved and fresh High dose (11 x 10^3 TH + cells; n = 5 and n = 4, respectively) and cryopreserved maximum feasible dose (MFD) (21 x 10^3 TH + cells; n = 3) (Fig. 3A). The MFD was calculated as the maximum number of neural microtissues that could be filled in the cavity formed by the cannula. All the animals were sacrificed at 5 months post-injection, except 2 rats from the MFD and vehicle groups each, kept for long-term observation and sacrificed at 8 months post-injection (data not shown). The number of TH + cells injected per animal was calculated by multiplying the number of injected microtissues and the number of TH + cells per microtissue specifically counted for each cryovial (Fig. 3A).

To demonstrate the functional capacity of the neural microtissues, we performed d-amphetamine-induced rotation testing at baseline (minimum 3 weeks after 6-OHDA lesioning) and every 4 weeks following transplantation. Hemiparkinsonian rats demonstrated functional recovery at 16 weeks post-transplantation for both cryopreserved and fresh High ($p < 0.001$, $p < 0.0001$, respectively), as well as cryopreserved MFD ($p < 0.0001$) (Fig. 3B). A delay was observed for the low dose group, with no significant effect 16 weeks post-transplantation in comparison to the excipient group, as demonstrated by a two-way ANOVA with Tukey's post hoc testing ($p = 0.36$). For this later group, functional recovery was observed 20 weeks post-transplantation ($p < 0.0001$). A significant improvement was observed at 12 weeks post-transplantation for the fresh High dose ($p < 0.05$). However, it did not achieve functional recovery before 16 weeks post-transplantation, defined by passing below the threshold of 2 rotations per minute. This demonstrates that the functional capacity of cryopreserved and fresh neural microtissues is equivalent.

Post-mortem histological characterisation

To evaluate the cellular composition of the graft, we performed immunofluorescent labelling of coronal sections of the graft. The presence of surviving human cells 5 months post-transplantation was confirmed with the human marker Stem121 (Fig. 3C b,f,j,n). Additionally, dopaminergic neurons were confirmed in the graft, with the majority of TH + cells located at the periphery of the graft (Fig. 3C c,g,k,o), as described previously with the use of foetal tissue [33] or hPSC-derived DA progenitors [9,11,12,34]. Fibres positive for both TH and the human marker Stem121 were detected emerging from the graft and reinnervating the striatum in all dose groups, cryopreserved or fresh (Fig. 3C b, c). This reinnervation was highlighted by image analysis using skeletonisation (Fig. 3C d,h,l,p).

Discussion

The *in vivo* study of iPSC-derived DA progenitors obtained from dual SMAD inhibition has been performed for more than a decade now [6–8]. It is noteworthy that every research group performing non-clinical studies observed an increase in the Time-to-Effect across studies, starting from 12 weeks [7] and 18 weeks [6], and recently ending at 24–26 weeks [9] and 28 weeks [11] in the latest efficacy studies before clinical translation. Although it is nearly impossible to attribute this delay to a unique parameter, two parameters can be considered potentially impactful: the implementation of GMP (Good Manufacturing Practices) and the transition to cryopreserved cells. Interestingly, the Time-To-Effect of the initiative led by the Center for iPS Cell Research and Application (CiRA, Japan) remained constant, achieving functional recovery at 16 weeks post-transplantation before implementation of the cryopreservation [8,10,35]. Their recent implementation of a cryopreservation step caused a delay in their Time-to-Effect, switching to 20 weeks post-transplantation [18]. While the fresh dose group in the present study showed a significant improvement at 12 weeks post-transplantation, it reached functional recovery only at 16 weeks after transplantation, resulting in no delay of the Time-to-Effect with cryopreserved cells. Our study marks the first grafting of cryopreserved 3D cell format containing DA progenitors and neurons, leading to a functional recovery observed at 16 weeks post-transplantation. However, it is important to acknowledge that the present *in vivo* study constitutes a proof-of-concept with a limited number of animals. This study serves as a tool to verify the functionality of the cells produced in a stirred tank bioreactor (STBR). Additional studies with more animals will be required, specifically to demonstrate the safety of the cell therapy product.

The precise mechanism of action underlying PD cell therapy has not been fully elucidated to date. A study has emphasised the necessity of obtaining appropriate A9 neurons after *in situ* differentiation, crucial for the correct reinnervation of the dorsal striatum and subsequent behavioural recovery in lesioned animals [36]. An additional optogenetics study confirmed the causal role of engrafted DA neuron depolarisation and dopamine release in this pharmacological effect [37]. Nevertheless, to obtain these A9 neurons after *in situ* differentiation, the absolute purity of the grafted midbrain DA progenitors may not be the ideal approach. Recently, the co-grafting of midbrain DA progenitors and forebrain progenitors in a dose-range study led to a better yield of TH + cells *in situ* compared to the use of midbrain dopaminergic progenitors alone [9]. It is noteworthy that one of the shortest time-to-effect observed is linked to a 3D format [10], with a behavioural recovery at 16 weeks post-transplantation, as in our study. This format may enhance cell diversity, potentially contributing to functional recovery. However, the proper characterisation of 3D format has not yet been performed using unbiased single-cell transcriptomics analysis. It will be interesting to use the most recent single-cell technologies previously used for graft characterisation [30,38]. This would allow us to better characterise 3D objects and further investigate each cell type's role and potential synergic roles in co-grafting. Finally, a similar time-to-effect than the one observed in the present study was recently achieved using cryopreserved single-cell suspension, with a functional recovery at 4 months post-transplantation [34]. While the unbiased single-cell transcriptomics analysis of the grafted cells was not performed, the flow cytometry results demonstrated lower purity than previous single-cell-based studies, with approximately 70% of the total cells double positive for FOXA2/LMX1A. This supports the hypothesis that cell diversity is potentially beneficial for functional recovery.

The optimal maturity stage of grafted cells remains unclear. Initial studies suggested that more mature cell types corresponding to immature neurons would be beneficial [39,40]. However, a recent study demonstrated that day 17 was the optimal maturity stage considering reinnervation capacity, quantified by the TH optical density unit (ODU) [34]. Notably, neither the number of TH + cells nor the behavioural recovery significantly differed between day 17 and day 24 cells. Day 17, however, exhibited higher variability in reinnervation and DA neuron yield compared to D24. Furthermore, using a single-cell suspension introduces a bias in identifying the optimal maturity stage, as the survivability of the cells may become the overriding factor rather than their inherent

capacity for reinnervation. More mature neurons are indeed particularly sensitive to mechanical or enzymatic dissociation [17]. The presence of TH + DA neurons in the neural microtissues characterised in the present study, as well as in 3D objects from another study associated with the same time-to-effect of 16 weeks after transplantation [10], may have a role in functionality, directly or indirectly by influencing *in situ* differentiation of the DA progenitors. Alternatively, better preservation of the cell microenvironment enabled by engraftment of 3D microtissue might favour cell functionality *in situ*.

Previous studies using the 3D format incorporated maturation phases in the neurodifferentiation protocol, yielding dopaminergic neurons before grafting [10,18], like in our study. However, extended maturation time until day 42 did not lead to behavioural recovery [8]. A recent study using 3D neurospheroids composed of directly reprogrammed dopaminergic neurons (iN) did not include any behavioural recovery data [15]. Regarding cellular diversity, it is also possible that interactions between the different cell types could occur. As the co-grafting of forebrain progenitors and midbrain DA progenitor increased the yield of DA neurons, one could imagine an interaction between midbrain DA progenitors and immature DA neurons when co-grafted. As too mature cell types are not preferable for the functionality, there might be a delicate equilibrium between DA progenitor and immature DA neurons, where the transplantation method, the format, the cryopreservation, and the cellular diversity may have complex and interacting effects. In the present study, we demonstrated that both DA Progenitors and DA neurons were present in the neural microtissues using immunofluorescent microscopy. It is not excluded that both cell types, in a 3D format, might have played a role in the mechanism of action. It would be interesting to precisely modify the composition of the neural microtissue to further investigate the role of each cell type in the future. Finally, Stem121-positive and TH-negative cells were detected in our grafts. These human non-dopaminergic cells require further characterisation to evaluate the safety of the cell product, along with a GLP-qualified safety study, which results are expected end of 2025.

Currently, all clinically translated neurodifferentiation processes for the obtention of hPSC-derived DA progenitor cells rely on 2D culture [9,11,12]. To enhance production volume sufficient for clinical trials, a scale-out approach was favoured [19,20]. This scale-out approach consists of multiplying the number of culture units in parallel. This contrasts with a scale-up approach, where the culture system is modified to increase the total volume produced per culture unit. Bioreactors are typically employed for scale-up, enhancing productivity and reducing costs [21]. While the scale achieved by previous protocols is sufficient for initiating clinical trials, it is important to anticipate scalable solutions compatible with potential downstream commercial phases. Additionally, 2D culture-based bioproduction processes are laborious and prone to variability as they are not automatised and rely on manual handling by operators. The present work is the first bioproduction of cell therapy for Parkinson's disease in a scalable bioreactor to the best of our knowledge. This study has been conducted using a single cell line. Future investigations should explore whether this bioproduction method enhances reproducibility across various cell lines.

Funding

This study was funded by Treefrog Therapeutics. This study received financial support from the French government in the framework of the Deeptech, FEDER (European fund) and AAP France 2030 programs. NPR received a PhD fellowship through the CIFRE program (Convention Industrielle de Formation par la Recherche) supported by the Association Nationale de la Recherche et de la Technologie.

Authors Contributions

NPR wrote the manuscript. NPR, LCE, MAB, BGU, FMO, ELU, LMA, MLF, TDU, JSC, KAL, EBE, EFA, MFE participated in the experimental design.

HWU, LPO, MDE, AJO, JPL, ELU performed the encapsulation and the bioreactor cultures. LMI and PMO performed the cryopreservation.

CMO, VDL, MLA and HCA performed the imaging of the neural microtissues. CMO performed the in vitro quantification of DA neurons. KSC, SGU and LPI performed and participated in the analysis of the flow cytometry. LPI and SGU participated in the *in vitro* transcriptomics analysis. NPR, MAB, MLE, LCE and BGU participated in the analysis of the *in vitro* imaging. NPR and LCE participated in all the *in vitro* data analyses.

ASO and JHA assisted in the design of the *in vivo* study. IJN and AMH developped and prepared the administration medium. NPR, MAB and GDA performed the transplantations of the *in vivo* study. GDA performed the behavioural analysis and the sacrifices. MLE, NPU, CMO, VDL and BGU performed the histological post-mortem imaging. NPR, EFA and TDU participated in the behavioural data analysis. NPR, BGU, MAB, MLE, TDU and EFA participated in the post-mortem histological data analysis.

NPR, EFA, LCE, TDU, BGU, MFE and EBE participated in the critical analysis of the results and the review of the manuscript.

Declaration of competing interest

The authors declare the following financial interests/personal relationships which may be considered as potential competing interests: Nicolas Prudon reports financial support was provided by TreeFrog Therapeutics. Erwan Bezard reports a relationship with TreeFrog Therapeutics that includes: consulting or advisory. Maxime Feyeux has patent issued to University of Bordeaux. Kevin Alessandri has patent issued to University of Bordeaux. Erwan Bezard has patent issued to University of Bordeaux. If there are other authors, they declare that they have no known competing financial interests or personal relationships that could have appeared to influence the work reported in this paper.

Acknowledgements

The University of Bordeaux and the Centre National de la Recherche Scientifique (CNRS) provided infrastructural support for the *in vivo* study. Treefrog Therapeutics produced the neural microtissues and the *in vitro* characterisation. The confocal microscope and the slide scanner were used in the Bordeaux Imaging Center (BIC), a service unit of the CNRS-INSERM and Bordeaux University, member of the national infrastructure France BioImaging supported by the French National Research Agency (ANR-10-INBS-04). The authors thank the team from the Bordeaux Imaging Center (BIC) for technical assistance with the imaging and Juan Estaun-Panzano for help with the image analysis.

Appendix A. Supplementary data

Supplementary data to this article can be found online at https://doi.org/10.1016/j.neurot.2024.e00436.

References

[1] Li W, Englund E, Widner H, Mattsson B, Van Westen D, Lätt J, et al. Extensive graft-derived dopaminergic innervation is maintained 24 years after transplantation in the degenerating parkinsonian brain. Proc Natl Acad Sci 2016;113:6544–9.
[2] Olanow CW, Goetz CG, Kordower JH, Stoessl AJ, Sossi V, Brin MF, et al. A double-blind controlled trial of bilateral fetal nigral transplantation in Parkinson's disease. Ann Neurol 2003;54:403–14.
[3] Freed CR, Greene PE, Breeze RE, Tsai WY, DuMouchel W, Kao R, et al. Transplantation of embryonic dopamine neurons for severe Parkinson's disease. N Engl J Med 2001;344:710–9.
[4] Parmar M, Grealish S, Henchcliffe C. The future of stem cell therapies for Parkinson disease. Nat Rev Neurosci 2020;21:103–15.
[5] Chambers SM, Fasano CA, Papapetrou EP, Tomishima M, Sadelain M, Studer L. Highly efficient neural conversion of human ES and iPS cells by dual inhibition of SMAD signaling. Nat Biotechnol 2009;27:275–80.
[6] Kriks S, Shim J-W, Piao J, Ganat YM, Wakeman DR, Xie Z, et al. Dopamine neurons derived from human ES cells efficiently engraft in animal models of Parkinson's disease. Nature 2011;480:547–51.

[7] Kirkeby A, Grealish S, Wolf DA, Nelander J, Wood J, Lundblad M, et al. Generation of regionally specified neural progenitors and functional neurons from human embryonic stem cells under defined conditions. Cell Rep 2012;1:703–14.
[8] Doi D, Samata B, Katsukawa M, Kikuchi T, Morizane A, Ono Y, et al. Isolation of human induced pluripotent stem cell-derived dopaminergic progenitors by cell sorting for successful transplantation. Stem Cell Rep 2014;2:337–50.
[9] Kirkeby A, Nelander J, Hoban DB, Rogelius N, Bjartmarz H, Storm P, et al. Preclinical quality, safety, and efficacy of a human embryonic stem cell-derived product for the treatment of Parkinson's disease. STEM-PD. Cell Stem Cell 2023;30:1299–1314.e9.
[10] Doi D, Magotani H, Kikuchi T, Ikeda M, Hiramatsu S, Yoshida K, et al. Pre-clinical study of induced pluripotent stem cell-derived dopaminergic progenitor cells for Parkinson's disease. Nat Commun 2020;11:3369.
[11] Piao J, Zabierowski S, Dubose BN, Hill EJ, Navare M, Claros N, et al. Preclinical efficacy and safety of a human embryonic stem cell-derived midbrain dopamine progenitor product, MSK-DA01. Cell Stem Cell 2021;28:217–229.e7.
[12] Park S, Park CW, Eom JH, Jo M-Y, Hur H-J, Choi SK, et al. Preclinical and dose-ranging assessment of hESC-derived dopaminergic progenitors for a clinical trial on Parkinson's disease. Cell Stem Cell 2024;31:25–38.e8.
[13] Skidmore S, Barker RA. Challenges in the clinical advancement of cell therapies for Parkinson's disease. Nat Biomed Eng 2023;7:370–86.
[14] Gilmore AP. Anoikis. Cell Death Differ 2005;12:1473–7.
[15] Kajtez J, Nilsson F, Laurin K, Bruzelius A, Cepeda-Prado E, Birtele M, et al. Injectable 3D microcultures enable intracerebral transplantation of mature neurons directly reprogrammed from patient fibroblasts [Pre-print]. Neuroscience 2023 Dec. Available from, http://biorxiv.org/lookup/doi/10.1101/2023.12.10.570992.
[16] Rossen NS, Anandakumaran PN, Zur Nieden R, Lo K, Luo W, Park C, et al. Injectable Therapeutic Organoids Using Sacrificial Hydrogels. iScience 2020;23:101052.
[17] Marchionini DM, Collier TJ, Camargo M, McGuire S, Pitzer M, Sortwell CE. Interference with anoikis-induced cell death of dopamine neurons: implications for augmenting embryonic graft survival in a rat model of Parkinson's disease. J Comp Neurol 2003;464:172–9.
[18] Hiramatsu S, Morizane A, Kikuchi T, Doi D, Yoshida K, Takahashi J. Cryopreservation of induced pluripotent stem cell-derived dopaminergic neurospheres for clinical application. J Park Dis. 2022;12:871–84.
[19] Eaker S, Abraham E, Allickson J, Brieva TA, Baksh D, Heathman TRJ, et al. Bioreactors for cell therapies: current status and future advances. Cytotherapy 2017;19:9–18.
[20] Hourd P, Chandra A, Medcalf N, Williams DJ. Regulatory challenges for the manufacture and scale-out of autologous cell therapies. StemBook. The Stem Cell Research Community, StemBook. June 30, 2014. https://doi.org/10.3824/stembook.1.96.1.
[21] Zhang H, Kent DE, Albanna M, Lhu L, Sun XS, Eaker S, et al. Bioreactor technology for cell therapy manufacturing in regenerative medicine. Curr Stem Cell Rep 2021;7:212–8.
[22] Cohen PJR, Luquet E, Pletenka J, Leonard A, Warter E, Gurchenkov B, et al. Engineering 3D micro-compartments for highly efficient and scale-independent expansion of human pluripotent stem cells in bioreactors. Biomaterials 2023;295:122033.
[23] Alessandri K, Sarangi BR, Gurchenkov VV, Sinha B, Kießling TR, Fetler L, et al. Cellular capsules as a tool for multicellular spheroid production and for investigating the mechanics of tumor progression in vitro. Proc Natl Acad Sci. 2013;110:14843–8.
[24] Alessandri K, Feyeux M, Gurchenkov B, Delgado C, Trushko A, Krause K-H, et al. A 3D printed microfluidic device for production of functionalized hydrogel microcapsules for culture and differentiation of human Neuronal Stem Cells (hNSC). Lab Chip 2016;16:1593–604.
[25] Chomczynski P, Sacchi N. Single-step method of RNA isolation by acid guanidinium thiocyanate-phenol-chloroform extraction. Anal Biochem 1987;162:156–9.
[26] Bustin SA, Benes V, Garson JA, Hellemans J, Huggett J, Kubista M, et al. The MIQE guidelines: minimum information for publication of quantitative real-time PCR experiments. Clin Chem 2009;55:611–22.
[27] Xie F, Xiao P, Chen D, Xu L, Zhang B. miRDeepFinder: a miRNA analysis tool for deep sequencing of plant small RNAs. Plant Mol Biol 2012;80:75–84.
[28] Ungerstedt U, Arbuthnott GW. Quantitative recording of rotational behavior in rats after 6-hydroxy-dopamine lesions of the nigrostriatal dopamine system. Brain Res 1970;24:485–93.
[29] Soria FN, Paviolo C, Doudnikoff E, Arotcarena M-L, Lee A, Danné N, et al. Synucleinopathy alters nanoscale organization and diffusion in the brain extracellular space through hyaluronan remodeling. Nat Commun 2020;11:3440.
[30] Tiklová K, Nolbrant S, Fiorenzano A, Björklund ÅK, Sharma Y, Heuer A, et al. Single cell transcriptomics identifies stem cell-derived graft composition in a model of Parkinson's disease. Nat Commun 2020;11:2434.
[31] Fiorenzano A, Sozzi E, Birtele M, Kajtez J, Giacomoni J, Nilsson F, et al. Single-cell transcriptomics captures features of human midbrain development and dopamine neuron diversity in brain organoids. Nat Commun 2021;12:7302.
[32] Denisenko E, Guo BB, Jones M, Hou R, de Kock L, Lassmann T, et al. Systematic assessment of tissue dissociation and storage biases in single-cell and single-nucleus RNA-seq workflows. Genome Biol 2020;21:130.
[33] Thompson L, Barraud P, Andersson E, Kirik D, Björklund A. Identification of dopaminergic neurons of nigral and ventral tegmental area subtypes in grafts of fetal ventral mesencephalon based on cell morphology, protein expression, and efferent projections. J Neurosci 2005;25:6467–77.
[34] Hiller BM, Marmion DJ, Thompson CA, Elliott NA, Federoff H, Brundin P, et al. Optimizing maturity and dose of iPSC-derived dopamine progenitor cell therapy for Parkinson's disease. Npj Regen Med 2022;7:24.
[35] Kikuchi T, Morizane A, Doi D, Okita K, Nakagawa M, Yamakado H, et al. Idiopathic Parkinson's disease patient-derived induced pluripotent stem cells function as midbrain dopaminergic neurons in rodent brains. J Neurosci Res 2017;95:1829–37.
[36] Grealish S, Diguet E, Kirkeby A, Mattsson B, Heuer A, Bramoulle Y, et al. Human ESC-derived dopamine neurons show similar preclinical efficacy and potency to fetal neurons when grafted in a rat model of Parkinson's disease. Cell Stem Cell 2014;15:653–65.
[37] Steinbeck JA, Choi SJ, Mrejeru A, Ganat Y, Deisseroth K, Sulzer D, et al. Optogenetics enables functional analysis of human embryonic stem cell–derived grafts in a Parkinson's disease model. Nat Biotechnol 2015;33:204–9.
[38] Rájová J, Davidsson M, Avallone M, Hartnor M, Aldrin-Kirk P, Cardoso T, et al. Deconvolution of spatial sequencing provides accurate characterization of hESC-derived DA transplants in vivo. Mol Ther - Methods Clin Dev 2023;29:381–94.
[39] Ganat YM, Calder EL, Kriks S, Nelander J, Tu EY, Jia F, et al. Identification of embryonic stem cell–derived midbrain dopaminergic neurons for engraftment. J Clin Invest 2012;122:2928–39.
[40] Qiu L, Lim YM, Chen AK, Reuveny S, Oh SKW, Tan EK, et al. Microcarrier-expanded neural progenitor cells can survive, differentiate, and innervate host neurons better when transplanted as aggregates. Cell Transplant 2016;25:1343–57.